

# Sliding Mode Attitude Maneuver Control for Rigid Spacecraft without Unwinding

Rui-Qi Dong, *Student Member, IEEE*, Ai-Guo Wu, *Member, IEEE* and Ying Zhang,

**Abstract**—In this paper, attitude maneuver control without unwinding phenomenon is investigated for rigid spacecraft. First, a novel switching function is constructed by a hyperbolic sine function. It is shown that the spacecraft system possesses the unwinding-free performance when the system states are on the sliding surface. Based on the designed switching function, a sliding mode controller is developed to ensure the robustness of the attitude maneuver control system. Another essential feature of the presented attitude control law is that a dynamic parameter is introduced to guarantee the unwinding-free performance when the system states are outside the sliding surface. The simulation results demonstrate that the unwinding phenomenon is avoided during the attitude maneuver of a rigid spacecraft by adopting the constructed switching function and the proposed attitude control scheme.

**Index Terms**—Modified Rodrigues Parameter, rigid spacecraft, sliding mode control, unwinding phenomenon.

## I. INTRODUCTION

Attitude maneuver control of rigid spacecraft has gained a great deal of attention in the last decades due to the benefits attained through its wide applications such as satellite communication, ocean surveillance, and spacecraft pointing [1]. Many control strategies have been proposed for solving the attitude maneuver control problem, such as optimal control [2], event trigger control [3], linear parameter varying control [4], model predictive control [5], backstepping control [6], and so on. However, the attitude controller design is still challenging due to two aspects: the inherent nonlinearity of the spacecraft attitude dynamics and the unwinding phenomenon during spacecraft attitude maneuver.

Sliding Mode Control (SMC) has been widely applied to deal with the nonlinearity of the spacecraft attitude dynamics due to its strong robustness to disturbance [7]–[11]. By using the integral sliding mode, a high-order sliding mode controller was proposed in [8] to address the chattering issue of SMC methods. In [9], an adaptive law was proposed to estimate the upper bound of the unknown lumped disturbances, including external disturbance, flexible vibration, and inertia uncertainty. In [10], a finite time controller was presented for attitude synchronization. In order to resolve the singular problem of the traditional terminal and faster terminal sliding-mode control designs, a nonsingular finite-time control approach was developed in [11].

This paragraph of the first footnote will contain the date on which you submitted your brief for review. It will also contain support information, including sponsor and financial support acknowledgment. For example, “This work was supported in part by the U.S. Department of Commerce under Grant BS123456.”

The next few paragraphs should contain the authors’ current affiliations, including current address and e-mail. For example, F. A. Author is with the National Institute of Standards and Technology, Boulder, CO 80305 USA (e-mail: author@boulder.nist.gov).

S. B. Author, Jr., was with Rice University, Houston, TX 77005 USA. He is now with the Department of Physics, Colorado State University, Fort Collins, CO 80523 USA (e-mail: author@lamar.colostate.edu).

T. C. Author is with the Electrical Engineering Department, University of Colorado, Boulder, CO 80309 USA, on leave from the National Research Institute for Metals, Tsukuba, Japan (e-mail: author@nrim.go.jp).

In the above control schemes, the unit quaternion was adopted to describe spacecraft attitude. However, the quaternion has four parameters, which can result in an extra constraint because three parameters are enough to describe the spacecraft attitude [12]. Thus, the Modified Rodrigues Parameter (MRP) was adopted to represent the spacecraft attitude, and plenty of controllers were proposed [13]–[16]. In [13], two finite-time attitude control laws were developed for single and multiple spacecraft, respectively. An attitude stabilization control law without angular velocity measurements was established for rigid spacecraft in [14]. The attitude maneuver control was investigated in [15], and a backstepping based adaptive sliding mode control strategy was proposed. In [16], a sliding mode control method was presented to solve the attitude tracking problem of rigid spacecraft.

Note that the unwinding problem was neglected by the aforementioned researches when the MRP was adopted to represent the spacecraft attitude. A typical feature of the MRP is its non-uniqueness, that is, a specific spacecraft orientation can be represented by two different MRP vectors. These two MRP vectors correspond to two different rotation angles and opposite rotation directions about the same Euler axis. The sum of these two rotation angles is  $2\pi$ . The unwinding phenomenon is that the rotation angle larger than  $\pi$  is performed by an attitude maneuver controller, which results in extra control effort. Nevertheless, to the best knowledge of the author, there is no unwinding-free result about the attitude maneuver control for the rigid spacecraft based on the MRP description.

Based on the above discussions, we aim to design an unwinding-free sliding mode attitude maneuver control law for a rigid spacecraft based on MRP representation. First of all, a switching function is designed using a hyperbolic sine function. Rigorous proof about the unwinding-free performance of the spacecraft system when the system states are on the sliding surface is given. Secondly, a sliding mode control law is presented to guarantee that all the system states arrive at the constructed sliding surface. Furthermore, it is proven that the unwinding-free performance of the proposed controller with a dynamic parameter is achieved before the system states reach the sliding surface. Finally, the simulations are performed to show the unwinding-free performance of the proposed controller. Compared with the SMC control law in [16], the proposed control law in this paper possesses faster convergence rate, and smaller control torque.

Throughout this paper, we use the italic-font notation for a scalar variable (as  $\rho$ ), the bold-font notation for a vector (as  $\sigma$ ), and the capital-letter notation for a matrix (as  $M$ ). The set of  $n$ -dimensional real vectors, and the set of  $m$ -by- $n$  real matrices, are denoted by  $\mathbb{R}^n$  and  $\mathbb{R}^{m \times n}$ , respectively. In addition,  $\mathbf{0}$  and  $I_3$  respectively denote a 3-dimensional zero vector and a  $3 \times 3$  identity matrix. We use  $\|\cdot\|$  to represent the 2-norm of a vector, and  $\otimes$  to represent the MRP multiplication. Moreover, the following two hyperbolic functions are used,  $\cosh x = \frac{e^x + e^{-x}}{2}$  and  $\sinh x = \frac{e^x - e^{-x}}{2}$  for  $x \in \mathbb{R}$ . Moreover, the following

relations are used:  $\frac{d(\cosh x)}{dx} = \sinh x$ ,  $\frac{d(\sinh x)}{dx} = \cosh x$ ,  $\frac{d(\tan x)}{dx} = \frac{1}{x^2+1}$ , and  $\cos^2 x = \frac{1}{\tan^2 x + 1}$ .

## II. MATHEMATIC MODEL

Before given the mathematical model, we first give some denotations. For any vector  $\mathbf{x} = [x_1 \ x_2 \ x_3]^T \in \mathbb{R}^3$ , let

$$\mathbf{x}^\times = \begin{bmatrix} 0 & -x_3 & x_2 \\ x_3 & 0 & -x_1 \\ -x_2 & x_1 & 0 \end{bmatrix},$$

and

$$M(\mathbf{x}) = \frac{(1 - \|\mathbf{x}\|^2) I_3 + 2\mathbf{x}^\times + 2\mathbf{x}\mathbf{x}^T}{4}. \quad (1)$$

### A. Attitude kinematics and dynamics

By using the Modified Rodrigues Parameter (briefly, MRP), the rigid spacecraft attitude dynamics can be given as [3]

$$\begin{cases} \dot{\boldsymbol{\sigma}} = M(\boldsymbol{\sigma})\boldsymbol{\omega}, \\ J\dot{\boldsymbol{\omega}} = -\boldsymbol{\omega}^\times J\boldsymbol{\omega} + \mathbf{u} + \mathbf{d}, \end{cases} \quad (2)$$

where  $\boldsymbol{\sigma} \in \mathbb{R}^3$  is the spacecraft attitude of the body frame  $\mathcal{F}_b$  with respect to the inertia frame  $\mathcal{F}_I$ ,  $\boldsymbol{\omega} \in \mathbb{R}^3$  is the angular velocity expressed in  $\mathcal{F}_b$ ;  $J \in \mathbb{R}^{3 \times 3}$  is the inertia matrix,  $\mathbf{u} \in \mathbb{R}^3$  is the control input, and  $\mathbf{d} \in \mathbb{R}^3$  is the disturbance.

### B. Attitude error kinematics and dynamics

Let  $\boldsymbol{\sigma}_d \in \mathbb{R}^3$  denotes the spacecraft attitude of the desired frame  $\mathcal{F}_d$  with respect to the inertia frame  $\mathcal{F}_I$ , and  $\boldsymbol{\omega}_d \in \mathbb{R}^3$  denotes the attitude angular velocity expressed in the desired frame  $\mathcal{F}_d$ . In addition, denote  $\boldsymbol{\sigma}_e \in \mathbb{R}^3$  as the attitude error between the desired attitude  $\boldsymbol{\sigma}_d$  and the body attitude  $\boldsymbol{\sigma}_b$ . Then, the attitude error  $\boldsymbol{\sigma}_e$  can be given by

$$\begin{aligned} \boldsymbol{\sigma}_e &= \boldsymbol{\sigma} \otimes \boldsymbol{\sigma}_d^*, \\ &= \frac{(1 - \|\boldsymbol{\sigma}\|^2)\boldsymbol{\sigma}_d + (1 - \|\boldsymbol{\sigma}_d\|^2)\boldsymbol{\sigma} + 2\boldsymbol{\sigma}_d^\times \boldsymbol{\sigma}}{1 + \|\boldsymbol{\sigma}_d\|^2 \|\boldsymbol{\sigma}\|^2 + 2\boldsymbol{\sigma}_d^T \boldsymbol{\sigma}}, \end{aligned} \quad (3)$$

where  $\boldsymbol{\sigma}_d^* = -\boldsymbol{\sigma}_d$ . Denote  $\boldsymbol{\omega}_e \in \mathbb{R}^3$  as the attitude angular velocity error between  $\boldsymbol{\omega}_d$  and  $\boldsymbol{\omega}_b$ . Then, we have

$$\boldsymbol{\omega}_e = \boldsymbol{\omega} - R(\boldsymbol{\sigma}_e)\boldsymbol{\omega}_d, \quad (4)$$

where  $R(\boldsymbol{\sigma}_e)$  is the rotation matrix from the desired frame  $\mathcal{F}_d$  to the body frame  $\mathcal{F}_b$ , and can be expressed as

$$R(\boldsymbol{\sigma}_e) = I_3 + \frac{8\boldsymbol{\sigma}_e^\times \boldsymbol{\sigma}_e^\times - 4(1 - \|\boldsymbol{\sigma}_e\|^2)\boldsymbol{\sigma}_e^\times}{(1 + \|\boldsymbol{\sigma}_e\|^2)^2}.$$

Thus, the attitude error kinematics can be obtained as [3]

$$\dot{\boldsymbol{\sigma}}_e = M(\boldsymbol{\sigma}_e)\boldsymbol{\omega}_e. \quad (5)$$

In addition, the rotation matrix  $R(\boldsymbol{\sigma}_e)$  satisfies  $\dot{R}(\boldsymbol{\sigma}_e) = -\boldsymbol{\omega}_e^\times R(\boldsymbol{\sigma}_e)$ . It follows from (4) that

$$\dot{\boldsymbol{\omega}}_e = \dot{\boldsymbol{\omega}} - R(\boldsymbol{\sigma}_e)\dot{\boldsymbol{\omega}}_d + \boldsymbol{\omega}_e^\times R(\boldsymbol{\sigma}_e)\boldsymbol{\omega}_d. \quad (6)$$

For a rest-to-rest attitude maneuver control problem, the desired angular velocity  $\boldsymbol{\omega}_d$  satisfies  $\boldsymbol{\omega}_d = \mathbf{0}$  and  $\dot{\boldsymbol{\omega}}_d = \mathbf{0}$ . Thus, it can be obtained from (6) that  $\dot{\boldsymbol{\omega}}_e = \dot{\boldsymbol{\omega}}$  holds. By substituting this relation into the second equation of (2), and using (5), the following rest-to-rest attitude maneuver error dynamics for a rigid spacecraft based on MRP can be obtained [15],

$$\begin{cases} \dot{\boldsymbol{\sigma}}_e = M(\boldsymbol{\sigma}_e)\boldsymbol{\omega}_e, \\ J\dot{\boldsymbol{\omega}}_e = -\boldsymbol{\omega}_e^\times J\boldsymbol{\omega}_e + \mathbf{u} + \mathbf{d}, \end{cases} \quad (7)$$

where the matrix  $M(\boldsymbol{\sigma}_e)$  in terms of  $\boldsymbol{\sigma}_e$  can be obtained by replacing  $\mathbf{x}$  with  $\boldsymbol{\sigma}_e$  in (1).

In addition, according to the Euler's principle rotation theorem [17], the rest-to-rest attitude maneuver of a rigid spacecraft can also be described as that the spacecraft performs a rotation from the body frame  $\mathcal{F}_b$  to the desired frame  $\mathcal{F}_d$  about a certain Euler axis, which is a unit vector. Suppose that the rotation angle and the Euler axis of this rotation are denoted by  $\theta(t) \in \mathbb{R}$  and  $\mathbf{e} \in \mathbb{R}^3$ , respectively. Then, the rest-to-rest attitude maneuver error  $\boldsymbol{\sigma}_e$  from  $\mathcal{F}_b$  to  $\mathcal{F}_d$  can be expressed as

$$\boldsymbol{\sigma}_e = \mathbf{e} \tan \frac{\theta(t)}{4}. \quad (8)$$

According to (3),  $\boldsymbol{\sigma}_e(0)$  can be obtained as long as the initial attitude  $\boldsymbol{\sigma}(0)$  of  $\boldsymbol{\sigma}$  and the desired attitude  $\boldsymbol{\sigma}_d$  are given. Thus, the following relations can be obtained by (8),

$$\theta(t) = 4 \arctan \mathbf{e}^T \boldsymbol{\sigma}_e, \quad (9)$$

and

$$\mathbf{e} = \frac{\boldsymbol{\sigma}_e(0)}{\|\boldsymbol{\sigma}_e(0)\|}. \quad (10)$$

The initial value  $\theta(0)$  of  $\theta(t)$  can be obtained by (9). By designing an attitude maneuver controller, the rigid spacecraft is driven to rotate about the fixed Euler axis  $\mathbf{e}$  in (10), such that the rotation angle  $\theta(t)$  converges from the initial value  $\theta(0)$  to approach 0 or  $2\pi$ .

### C. Unwinding phenomenon

The phenomenon that spacecraft performs a rotation angle larger than  $\pi$  to arrive at the desired attitude is called the "unwinding". For the rest-to-rest attitude maneuver error dynamics of a rigid spacecraft described by (7) with (9),  $\theta(t) = 0$  and  $\theta(t) = 2\pi$  represent the same attitude. However, the existing attitude maneuver control schemes are designed to ensure that the rotation angle  $\theta(t)$  converges from any initial value  $\theta(0)$  to 0. In this case, if  $\theta(0) > \pi$ , then the spacecraft is driven to perform a rotation larger than  $\pi$  about the Euler axis  $\mathbf{e}$ , which results in the unwinding phenomenon. However, the rigid spacecraft can reach the desired attitude by rotating an angle  $2\pi - \theta(0)$ , which is smaller than  $\pi$ , about the Euler axis  $\mathbf{e}$  in the opposite direction.

### D. Control objective

The control task in this work is to design an unwinding-free attitude sliding mode controller for the attitude maneuver error dynamics (7) with (9) of a rigid spacecraft, such that the following relations hold,

$$\lim_{t \rightarrow \infty} \theta(t) = 0 \text{ or } \lim_{t \rightarrow \infty} \theta(t) = 2\pi, \quad \lim_{t \rightarrow \infty} \boldsymbol{\omega}_e = \mathbf{0}. \quad (11)$$

Moreover, the unwinding phenomenon is also avoided.

## III. CONTROLLER DESIGN METHODS

In this section, we aim to develop an unwinding-free attitude controller for the system (7), using sliding mode control theory. To facilitate the controller development, we give some lemmas in subsection III-A. To avoid the unwinding phenomenon when the system states are on the sliding surface, we construct a novel switching function in subsection III-B. In order to avoid the unwinding phenomenon before the system states reach the sliding surface, a sliding mode control law with a dynamic parameter is developed in subsection III-C.

### A. Some lemmas

**Lemma 1:** Consider the rotation angle  $\theta(t)$  given by (9). The following relation holds,

$$\dot{\theta}(t) = e^T \omega_e, \quad (12)$$

where the attitude angular velocity error  $\omega_e$  is defined in (4), and the Euler axis  $e$  can be obtained from (10).

**Proof.** Taking the derivative of both sides of (9), and using the first relation of (7), yields

$$\begin{aligned} \dot{\theta}(t) &= \frac{4e^T \dot{\sigma}_e}{1 + (e^T \sigma_e)^2} \\ &= \frac{4e^T M(\sigma_e) \omega_e}{1 + (e^T \sigma_e)^2}. \end{aligned} \quad (13)$$

In addition, by replacing  $x$  with  $\sigma_e$  in (1), and using (8), we have

$$\begin{aligned} e^T M(\sigma_e) &= \frac{(1 - \|\sigma_e\|^2) e^T + 2e^T e^\times \tan \frac{\theta(t)}{4} + 2e^T \tan^2 \frac{\theta(t)}{4}}{4} \\ &= \frac{(1 - \tan^2 \frac{\theta(t)}{4}) e^T + 2e^T \tan^2 \frac{\theta(t)}{4}}{4} \\ &= \frac{(1 + \tan^2 \frac{\theta(t)}{4}) e^T}{4}. \end{aligned} \quad (14)$$

It follows from (8) and (13) that

$$\begin{aligned} \dot{\theta}(t) &= \frac{4}{1 + \sigma_e^T \sigma_e} \frac{1 + \|\sigma_e\|^2}{4} e^T \omega_e \\ &= e^T \omega_e. \end{aligned}$$

Thus, the proof is completed. ■

**Lemma 2:** Suppose  $V(x)$  is a  $C^1$  smooth positive-definite function (defined on  $U \subset \mathbb{R}^n$ ) and  $\dot{V}(x) + \lambda V^\alpha(x)$  is a negative semi-definite function on  $U \subset \mathbb{R}^n$  for  $\alpha \in (0, 1)$  and  $\lambda \in \mathbb{R}^+$ , then there exists an area  $U_0 \subset \mathbb{R}^n$  such that any  $V(x)$  which starts from  $U_0 \subset \mathbb{R}^n$  can reach  $V(x) \equiv 0$  in finite time. Moreover, if  $T_s$  is the time needed to reach  $V(x) \equiv 0$ , then

$$T_s \leq \frac{V^{1-\alpha}(x_0)}{\lambda(1-\alpha)},$$

where  $V(x_0)$  is the initial value of  $V(x)$ .

### B. Switching function

For the rest-to-rest attitude maneuver error dynamics (7) with (9) of a rigid spacecraft, the switching function is designed as

$$s = \omega_e - \alpha \rho(\sigma_e) \sigma_e, \quad (15)$$

where  $\alpha$  is a positive number, and

$$\rho(\sigma_e) = \frac{\sinh g(\sigma_e)}{1 + \sigma_e^T \sigma_e}, \quad (16)$$

with

$$g(\sigma_e) = \arctan e^T \sigma_e - \frac{\pi}{4}. \quad (17)$$

Next, a theorem is given to demonstrate that the control goal in (11) can be achieved when  $\omega_e$  and  $\sigma_e$  are restricted to the sliding surface  $s = 0$ . Moreover, it is proven that the unwinding phenomenon is conquered on the sliding surface.

Before given the theorem, we should give some properties of the functions  $\cosh x$  and  $\sinh x$  for  $x \in [-\pi, \pi]$ . The minimum

value of the function  $\cosh x$  can be obtained when  $x = 0$ , and the maximum value of the function  $\cosh x$  can be obtained when  $x = -\pi$  or  $x = \pi$ . In addition, for  $x < 0$ ,  $\sinh x < 0$  holds, and for  $x \geq 0$ ,  $\sinh x \geq 0$  holds.

**Theorem 3:** Consider the rest-to-rest attitude maneuver error dynamics (7) with (9) for a rigid spacecraft. When the attitude errors  $\sigma_e$  and  $\omega_e$  are restricted to the sliding surface  $s = 0$ , the following conclusions are obtained.

(i) The unwinding phenomenon is avoided.

(ii) The control goal in (11) is attained.

**Proof.** Suppose that when  $t = t_{s0}$  the system states reach the sliding surface  $s = 0$ . Then, it can be obtained from (15) that

$$\omega_e = \alpha \rho(\sigma_e) \sigma_e. \quad (18)$$

To prove the conclusion (i), we need to prove that the following relations hold,

$$\lim_{t \rightarrow \infty} \theta(t) = \begin{cases} 0, & \text{if } \theta(t_{s0}) \in (0, \pi), \\ 2\pi, & \text{if } \theta(t_{s0}) \in (\pi, 2\pi). \end{cases} \quad (19)$$

It can be obtained from (12) and (18) that

$$\dot{\theta}(t) = \alpha e^T \rho(\sigma_e) \sigma_e. \quad (20)$$

In the following, we rewrite  $\dot{\theta}(t)$  in terms of the rotation angle  $\theta(t)$  and the Euler axis  $e$ . First, using (8) and (17),  $g(\sigma_e)$  is rewritten as

$$\begin{aligned} g(\theta(t)) &= \arctan e^T e \tan \frac{\theta(t)}{4} - \frac{\pi}{4} \\ &= \frac{\theta(t)}{4} - \frac{\pi}{4}. \end{aligned} \quad (21)$$

Applying (8) and (21) to (16), gives

$$\begin{aligned} \rho(\theta(t)) &= \frac{g(\theta(t))}{1 + e^T e \tan^2 \frac{\theta(t)}{4}} \\ &= \frac{\sinh \left( \frac{\theta(t)}{4} - \frac{\pi}{4} \right)}{1 + \tan^2 \frac{\theta(t)}{4}} \\ &= \sinh \left( \frac{\theta(t)}{4} - \frac{\pi}{4} \right) \cos^2 \frac{\theta(t)}{4}. \end{aligned} \quad (22)$$

It follows from (8) and (18) that  $\omega_e$  can be rewritten as

$$\omega_e = \alpha e \sinh \left( \frac{\theta(t)}{4} - \frac{\pi}{4} \right) \cos^2 \frac{\theta(t)}{4} \tan \frac{\theta(t)}{4}. \quad (23)$$

Following (8), (12) and (23), one can obtain

$$\dot{\theta}(t) = \alpha \sinh \left( \frac{\theta(t)}{4} - \frac{\pi}{4} \right) \cos^2 \frac{\theta(t)}{4} \tan \frac{\theta(t)}{4}. \quad (24)$$

In addition, there hold  $\sinh \left( \frac{\theta(t)}{4} - \frac{\pi}{4} \right) < 0$  for  $\theta(t) \in (0, \pi)$ , and  $\sinh \left( \frac{\theta(t)}{4} - \frac{\pi}{4} \right) > 0$  for  $\theta(t) \in (\pi, 2\pi)$ . As  $\tan \frac{\theta(t)}{4} \geq 0$  for  $\theta(t) \in (0, 2\pi)$ , it can be derived from (24) that  $\dot{\theta}(t) < 0$  for  $\theta(t_{s0}) \in (0, \pi)$ ,  $\dot{\theta}(t) > 0$  for  $\theta(t_{s0}) \in (\pi, 2\pi)$ , and  $\dot{\theta}(t) = 0$  for  $\theta(t) = 0$  or  $\theta(t) = 2\pi$ . Thus, the relations in (19) is obtained. This implies that the unwinding phenomenon is conquered when the system states are sliding on the sliding surface  $s = 0$ .

Thus, (i) is proven.

Next, the fact that the control goal in (11) is achieved on the sliding surface  $s = 0$  is proven. For this end, we chose the following Lyapunov function,

$$V_1(t) = \kappa - \cosh g(\sigma_e), \quad (25)$$

where  $\kappa = \max(\cosh g(\sigma_e))$ . Substituting (21) into (25), yields

$$V_1(t) = \kappa - \cosh g(\theta(t)), \quad (26)$$

where

$$\kappa = \cosh(g(\theta(t)))|_{\theta=0} = \cosh(g(\theta(t)))|_{\theta=2\pi}.$$

The time derivative of  $V_1(t)$  in (26) along time is

$$\dot{V}_1(t) = -\frac{dg(\theta(t))}{dt} \sinh g(\theta(t)).$$

It follows from (21) and Lemma 1 that

$$\dot{V}_1(t) = -\frac{\dot{\theta}(t)}{4} \sinh\left(\frac{\theta(t)}{4} - \frac{\pi}{4}\right). \quad (27)$$

By substituting (23) into (27), we have

$$\dot{V}_1(t) = -\frac{\alpha}{4} \cos^2 \frac{\theta(t)}{4} \sinh^2\left(\frac{\theta(t)}{4} - \frac{\pi}{4}\right) \tan \frac{\theta(t)}{4}. \quad (28)$$

It is clear that  $\dot{V}_1(t) \leq 0$  because  $\tan \frac{\theta(t)}{4} \geq 0$  holds for  $\theta \in (0, 2\pi)$ .

Moreover, according to (28), we obtain that if  $\dot{V}_1(t) = 0$ , there hold

$$\cos^2 \frac{\theta(t)}{4} = 0,$$

or

$$\sinh^2\left(\frac{\theta(t)}{4} - \frac{\pi}{4}\right) = 0,$$

or

$$\tan \frac{\theta(t)}{4} = 0.$$

Thus, we have  $\theta(t) = 2\pi$  or  $\theta(t) = \pi$  or  $\theta(t) = 0$  if  $\dot{V}_1(t) = 0$ . In addition, it can be readily computed from (26) that the maximum value of  $V_1(t)$  is obtained at  $\theta = \pi$ , and the minimum value of  $V_1(t)$  is obtained at  $\theta(t) = 2\pi$  or  $\theta(t) = 0$ . Consequently, there holds

$$\lim_{t \rightarrow \infty} \theta(t) = 0 \text{ or } \lim_{t \rightarrow \infty} \theta(t) = 2\pi.$$

Further, in view of (23), we have  $\omega_e = \mathbf{0}$  for  $\theta(t) = 2\pi$  or  $\theta(t) = 0$ . This implies that the control goal (11) is achieved on the sliding surface  $s = \mathbf{0}$ .

Hence, the proof is completed. ■ By Theorem 3, it is proven that the unwinding phenomenon is avoided when the system states are on the sliding surface  $s = \mathbf{0}$ . In the subsequent subsection, it is shown that the unwinding-free performance of the closed-loop attitude maneuver system (7) is guaranteed by designing a sliding mode control law with a dynamic parameter.

### C. Unwinding-Free Sliding Mode Control Law

In this section, we need to construct a control law such that the condition  $s = \mathbf{0}$  is achieved in finite-time. This condition assures us that all the system states of the closed-loop attitude maneuver error dynamics (7) arrive at the sliding surface  $s = \mathbf{0}$  in finite-time. Moreover, the unwinding phenomenon is also avoided before the system states reach the sliding surface.

Consider a class of state feedback control for the rest-to-rest attitude maneuver error dynamics (7) with (9) of a rigid spacecraft in the following form,

$$\mathbf{u} = \mathbf{u}_{eq} + \mathbf{u}_n, \quad (29)$$

where  $\mathbf{u}_{eq}$  is the equivalent control term for the nominal system,  $\mathbf{u}_n$  is the switching control term, which is designed to deal with

the disturbance. Thus, the equivalent control  $\mathbf{u}_{eq}$  can be obtained from the nominal system part by setting  $\dot{s} = \mathbf{0}$ , such that

$$\dot{s} = \dot{\omega}_e - \alpha \dot{\rho}(\sigma_e) \sigma_e - \alpha \rho(\sigma_e) \dot{\sigma}_e = \mathbf{0}. \quad (30)$$

By setting  $\mathbf{d} = \mathbf{0}$ , the following nominal system part of (7) can be obtained,

$$J\dot{\omega}_e = -\omega_e^\times J\omega_e + \mathbf{u}.$$

Substituting the above equation into (30) obtains

$$\dot{s} = J^{-1}(-\omega_e^\times J\omega_e + \mathbf{u}_{eq}) - \alpha \dot{\rho}(\sigma_e) \sigma_e - \alpha \rho(\sigma_e) \dot{\sigma}_e = \mathbf{0}.$$

By solving the above equation concerning  $\mathbf{u}_{eq}$ , we have

$$\mathbf{u}_{eq} = \omega_e^\times J\omega_e + \alpha J \dot{\rho}(\sigma_e) \sigma_e + \alpha J \rho(\sigma_e) \dot{\sigma}_e.$$

In addition, the control term  $\mathbf{u}_n$  is designed as,

$$\mathbf{u}_n = -(\gamma_1 + \gamma_2(t)) \operatorname{sgn}(s), \quad (31)$$

where  $\gamma_1 \geq \|\mathbf{d}\|_{\max}$ ,  $\gamma_2(t)$  is a positive-valued function, and

$$\operatorname{sgn}(s) = \begin{bmatrix} \frac{s_1}{|s_1|} & \frac{s_2}{|s_2|} & \frac{s_3}{|s_3|} \end{bmatrix}^T.$$

By concluding previous derivations, the following unwinding-free sliding mode control (briefly, UFSMC) law is obtained,

$$\begin{cases} \mathbf{u} = \mathbf{u}_{eq} + \mathbf{u}_n, \\ \mathbf{u}_{eq} = \omega_e^\times J\omega_e + \alpha J \dot{\rho}(\sigma_e) \sigma_e + \alpha J \rho(\sigma_e) \dot{\sigma}_e, \\ \mathbf{u}_n = -(\gamma_1 + \gamma_2(t)) \operatorname{sgn}(s), \\ s = \omega_e - \alpha \rho(\sigma_e) \sigma_e, \\ \rho(\sigma_e) = \frac{\sinh g(\sigma_e)}{1 + \sigma_e^T \sigma_e}, \\ g(\sigma_e) = \arctan e^T \sigma_e - \frac{\pi}{4}, \\ e = \frac{\sigma_e(0)}{\|\sigma_e(0)\|}, \end{cases} \quad (32)$$

where  $\alpha$  is a positive number,  $\sigma_e(0)$  is the initial value of  $\sigma_e$ ,  $\gamma_1 \geq \|\mathbf{d}\|_{\max}$ , and  $\gamma_2(t)$  is a positive-valued function, which is given in the following theorem.

**Theorem 4:** Consider a rest-to-rest attitude maneuver problem of a rigid spacecraft described by (7) with (9). If the dynamic parameter  $\gamma_2(t)$  is chosen as

$$\gamma_2(t) = \frac{\alpha}{\lambda_{\min}(J^{-1})} \left| \dot{h}(t) \right|, \quad (33)$$

where  $\alpha > 0$ ,  $\lambda_{\min}(J^{-1})$  represents the minimum eigenvalue of the inverse matrix of  $J$ , and

$$h(t) = \rho(\sigma_e) \|\sigma_e\|, \quad (34)$$

with  $\rho(\sigma_e)$  defining in (16). Then, the following conclusions are acquired.

- (i) The switching function  $s$  converges to zero in finite time.
- (ii) The unwinding phenomenon is avoided before the system states reach the switching surface  $s = \mathbf{0}$ .

**Proof.** To prove (i), we chose the following Lyapunov function,

$$V_2(t) = \frac{1}{2} s^T s. \quad (35)$$

Taking time derivative of the above equation, and using (15), yields

$$\begin{aligned} \dot{V}_2(t) &= s^T \dot{s} \\ &= s^T (\dot{\omega}_e - \alpha \dot{\rho}(\sigma_e) \sigma_e - \alpha \rho(\sigma_e) \dot{\sigma}_e). \end{aligned}$$



Substituting the second equation of (7) and controller (32) into the above equation, we arrive at

$$\begin{aligned}\dot{V}_2(t) &= \mathbf{s}^T (J^{-1} (-\boldsymbol{\omega}_e^\times J \boldsymbol{\omega}_e + \mathbf{u} + \mathbf{d}) - \alpha \dot{\rho}(\boldsymbol{\sigma}_e) \boldsymbol{\sigma}_e \\ &\quad - \alpha \rho(\boldsymbol{\sigma}_e) \dot{\boldsymbol{\sigma}}_e) \\ &= -\mathbf{s}^T J^{-1} (\gamma_1 + \gamma_2(t)) \operatorname{sgn}(\mathbf{s}) + \mathbf{s}^T J^{-1} \mathbf{d} \\ &= -\gamma_2(t) \mathbf{s}^T J^{-1} \operatorname{sgn}(\mathbf{s}) - \mathbf{s}^T J^{-1} (\gamma_1 - \|\mathbf{d}\|) \\ &\leq -\gamma_2(t) \mathbf{s}^T J^{-1} \operatorname{sgn}(\mathbf{s}).\end{aligned}\quad (36)$$

Obviously, there holds

$$\mathbf{s}^T J^{-1} \operatorname{sgn}(\mathbf{s}) \geq \lambda_{\min}(J^{-1}) \|\mathbf{s}\|. \quad (37)$$

According to (37), one deduces from (36) that

$$\dot{V}_2(t) \leq -\gamma_2(t) \lambda_{\min}(J^{-1}) \|\mathbf{s}\|.$$

By (35) and (37), the above equation can be rewritten as

$$\begin{aligned}\dot{V}_2(t) &\leq -\sqrt{2} \gamma_2(t) \lambda_{\min}(J^{-1}) \left(\frac{1}{2} \mathbf{s}^T \mathbf{s}\right)^{\frac{1}{2}} \\ &= -\sqrt{2} \gamma_2(t) \lambda_{\min}(J^{-1}) V_2^{\frac{1}{2}}(t).\end{aligned}\quad (38)$$

Using Lemma 2, it is immediate to conclude that the switching function  $\mathbf{s}$  converges to zero in finite time.

Thus, (i) is proven.

Next, we prove that the unwinding-free performance is ensured by the developed controller (32) with (33) when the system states are outside the switching surface  $\mathbf{s} = \mathbf{0}$ .

It can be further derived from (38) that

$$\frac{\dot{V}_2(t)}{V_2^{\frac{1}{2}}(t)} \leq -\sqrt{2} \gamma_2(t) \lambda_{\min}(J^{-1}).$$

Suppose the initial time is  $t_0 = 0$ . By taking integral of both sides of the above equation, we have

$$\int_0^t \frac{\dot{V}_2(\tau)}{V_2^{\frac{1}{2}}(\tau)} d\tau \leq -\sqrt{2} \lambda_{\min}(J^{-1}) \int_0^t \gamma_2(\tau) d\tau,$$

or, equivalently,

$$V_2^{\frac{1}{2}}(t) \leq -\frac{\lambda_{\min}(J^{-1})}{\sqrt{2}} \int_0^t \gamma_2(\tau) d\tau + V_2^{\frac{1}{2}}(0). \quad (39)$$

Let

$$v(t) = \mathbf{e}^T \mathbf{s}. \quad (40)$$

Then, applying (15), (8), Lemma 1, and (34) to (40), yields

$$\begin{aligned}v(t) &= \mathbf{e}^T \boldsymbol{\omega}_e - \alpha \rho(\boldsymbol{\sigma}_e) \mathbf{e}^T \boldsymbol{\sigma}_e \\ &= \dot{v}(t) - \alpha \rho(\boldsymbol{\sigma}_e) \|\boldsymbol{\sigma}_e\| \\ &= \dot{v}(t) - \alpha h(t).\end{aligned}\quad (41)$$

In addition, it can be obtained from (40) that

$$\begin{aligned}v^2(t) &= (\mathbf{e}^T \mathbf{s})^T \mathbf{e}^T \mathbf{s} \\ &\leq \|\mathbf{e} \mathbf{e}^T\| \|\mathbf{s}\|^2 \\ &\leq \lambda_{\max}(\mathbf{e} \mathbf{e}^T) \|\mathbf{s}\|^2,\end{aligned}$$

where  $\lambda_{\max}(\mathbf{e} \mathbf{e}^T)$  is the maximum eigenvalue of the matrix  $\mathbf{e} \mathbf{e}^T$ . Note that the Euler axis  $\mathbf{e}$  is a unit vector, thus the matrix  $\mathbf{e} \mathbf{e}^T$  is an idempotent matrix. Consequently, we have  $\lambda_{\max}(\mathbf{e} \mathbf{e}^T) = 1$ . Then, it is clear that

$$v^2(t) \leq \|\mathbf{s}\|^2.$$

This together with (35), results in

$$\frac{1}{2} v^2(t) \leq V_2(t). \quad (42)$$

In this paper, the rest-to-rest attitude maneuver problem is considered, thus the initial attitude velocity is zero, i.e.,  $\boldsymbol{\omega}_e(0) = \mathbf{0}$ . Further, it can be obtained from (12) that  $\dot{\theta}(t) = 0$ . In this case, by (41), the initial value of  $v(t)$  can be obtained as

$$v(0) = -\alpha h(0). \quad (43)$$

As  $\boldsymbol{\omega}_e(0) = \mathbf{0}$ , then by (35), (15), (34), and (43), the initial value of  $V_2(0)$  can be obtained as

$$\begin{aligned}V_2(0) &= \frac{1}{2} \mathbf{s}^T(0) \mathbf{s}(0) \\ &= \frac{1}{2} \alpha^2 \rho^2(\boldsymbol{\sigma}_e(0)) \|\boldsymbol{\sigma}_e(0)\|^2 \\ &= \frac{1}{2} v^2(0).\end{aligned}\quad (44)$$

Substituting (42) and (44) into (39) gives

$$\begin{aligned}\left(\frac{1}{2} v^2(t)\right)^{\frac{1}{2}} \leq V^{\frac{1}{2}}(t) &\leq -\frac{\lambda_{\min}(J^{-1})}{\sqrt{2}} \int_0^t \gamma_2(\tau) d\tau \\ &\quad + \left(\frac{1}{2} v^2(0)\right)^{\frac{1}{2}},\end{aligned}\quad (45)$$

which can be rewritten as

$$|v(t)| \leq -\lambda_{\min}(J^{-1}) \int_0^t \gamma_2(\tau) d\tau + |v(0)|. \quad (46)$$

As  $\gamma_2(t) > 0$ , it can be obtained from (46) that  $v(t)$  will decrease to 0 when  $v(0) > 0$ , and  $v(t)$  will increase to 0 when  $v(0) < 0$ .

To prove the unwinding-free phenomenon of the proposed control law (32) with  $\gamma_2(t)$  being chosen in (33), we need to prove that  $\dot{\theta}(t) < 0$  for  $\theta(0) \in (0, \pi)$ , and  $\dot{\theta}(t) > 0$  for  $\theta(0) \in (\pi, 2\pi)$ . To this end, the following two cases are considered to complete the proof.

(1) When  $\theta(0) \in (0, \pi)$ , there holds  $\sinh\left(\frac{\theta(0)}{4} - \frac{\pi}{4}\right) < 0$ . Then, it can be obtained from (8), (22), and (34) that there holds  $h(0) = \rho(\theta(0)) \tan \frac{\theta(0)}{4} < 0$ . Further, according to (43),  $v(0) = -\alpha h(0) > 0$  holds. Thus,  $v(t)$  will decrease to zero. In such a case, by using (41) and (43), (46) can be rewritten as

$$\dot{v}(t) - \alpha h(t) \leq -\lambda_{\min}(J^{-1}) \int_0^t \gamma_2(\tau) d\tau - \alpha h(0).$$

It can be further rewritten as

$$\begin{aligned}\dot{v}(t) &\leq -\lambda_{\min}(J^{-1}) \int_0^t \gamma_2(\tau) d\tau - \alpha h(0) + \alpha h(t) \\ &= -\lambda_{\min}(J^{-1}) \int_0^t \gamma_2(\tau) d\tau + \alpha \int_0^t \frac{dh(\tau)}{d\tau} d\tau \\ &= -\int_0^t \left(\lambda_{\min}(J^{-1}) \gamma_2(\tau) - \alpha \dot{h}(\tau)\right) d\tau.\end{aligned}\quad (47)$$

If  $\dot{h}(t) > 0$ , then it can be obtained from (33) that  $\gamma_2(t) = \frac{\alpha \dot{h}(t)}{\lambda_{\min}(J^{-1})}$ . It is followed from (47) that  $\dot{v}(t) \leq 0$ .

If  $\dot{h}(t) < 0$ , then it can be obtained from (33) that  $\gamma_2(t) = -\frac{\alpha \dot{h}(t)}{\lambda_{\min}(J^{-1})}$ . With this, it can be derived from (47) that

$$\dot{v}(t) \leq 2\alpha \int_0^t \dot{h}(\tau) d\tau \leq 0.$$

Thus, it can be obtained from above two cases that when  $\theta(0) \in (0, \pi)$ , there holds  $\dot{\theta}(t) \leq 0$ .

(2) When  $\theta(0) \in (\pi, 2\pi)$ , there holds  $\sinh\left(\frac{\theta(0)}{4} - \frac{\pi}{4}\right) < 0$ . Then, it can be obtained from (8), (22), and (34) that there holds  $h(0) = \rho(\theta(0)) \tan \frac{\theta(0)}{4} > 0$ . Further, according to (43),

$v(0) = -\alpha h(0) < 0$  holds. Thus,  $v(t)$  will increase to zero. In such a case, by using (41) and (43), (46) can be rewritten as

$$-\dot{\theta}(t) + \alpha h(t) \leq -\lambda_{\min}(J^{-1}) \int_0^t \gamma_2(\tau) d\tau + \alpha h(0).$$

Then, the following equation can be further obtained,

$$\begin{aligned} \dot{\theta}(t) &\geq \lambda_{\min}(J^{-1}) \int_0^t \gamma_2(\tau) d\tau + \alpha h(t) - \alpha h(0) \\ &= \lambda_{\min}(J^{-1}) \int_0^t \gamma_2(\tau) d\tau + \alpha \int_0^t \frac{dh(\tau)}{d\tau} d\tau \\ &\geq \int_0^t \left( \lambda_{\min}(J^{-1}) \gamma_2(\tau) + \alpha \dot{h}(\tau) \right) d\tau. \end{aligned} \quad (48)$$

If  $\dot{h}(t) > 0$ , there holds  $\gamma_2(\tau) = \frac{\alpha \dot{h}(\tau)}{\lambda_{\min}(J^{-1})}$  according to (33). Substituting it into (48), we have

$$\dot{\theta}(t) \geq 2\alpha \int_0^t \dot{h}(\tau) d\tau \geq 0.$$

If  $\dot{h}(t) < 0$ , there holds  $\gamma_2(\tau) = -\frac{\alpha \dot{h}(\tau)}{\lambda_{\min}(J^{-1})}$  from (33). Substituting it into (48), we have  $\dot{\theta}(t) \geq 0$ .

Thus, it can be obtained from above two cases that when  $\theta(0) \in (\pi, 2\pi)$ , the rotation angle  $\theta(t)$  will increase to  $2\pi$ .

Based on the above discussion, the conclusion (ii) is proven. ■

In Theorem 4, the unwinding-free performance before the system states reach the switching surface is proven. In Theorem 3, the unwinding-free performance when the system states are constricted to the sliding surface is also shown. The results in these two theorems have illustrated that the proposed UFSMC law (32) has the unwinding-free property.

*Remark 1:* One drawback of the control law (31) is that it is discontinuous due to the discontinuousness of  $u_n$  about the sliding surface  $s = 0$ . This characteristic may cause an undesirable chattering phenomenon. For practical implementations, the controller must be smoothed. Thus, the discontinuous function  $\text{sgn}(s)$  is replaced by the smooth continuous function  $l(s) = [l(s_1) \ l(s_2) \ l(s_3)]^T$  with  $l(s_i)$  in the following equation,

$$l(s_i) = \begin{cases} \text{sgn}(s_i), & \text{if } |s_i| \geq \varepsilon_1, \\ \arctan\left(\frac{s_i \tan(1)}{\varepsilon_1}\right), & \text{if } |s_i| < \varepsilon_1, \end{cases} \quad i = 1, 2, 3, \quad (49)$$

where  $\varepsilon$  is a small positive value. As  $\varepsilon_1$  approaches zero, the performance of this boundary layer can be made arbitrarily close to that of original control law.

Another drawback of the proposed control law (32) is that it suffers the singular problem because  $\theta(t) = 2\pi$  is a singular point for  $\sigma_e$ , which may cause an unbounded control magnitude. This potential drawback can be resolved by introducing a boundary layer about  $\sigma_e$ , such that

$$\sigma_{ei} = \begin{cases} \frac{\text{sgn}(\sigma_{ei})}{\varepsilon_2}, & \text{if } \frac{1}{|\sigma_{ei}|} \leq \varepsilon_2, \\ \sigma_{ei}, & \text{if } \frac{1}{|\sigma_{ei}|} > \varepsilon_2, \end{cases}$$

where  $\varepsilon_2 > 0$ ,  $\sigma_{ei}$  is the  $i$ -th element of the vector  $\sigma_e$ , and

$$\text{sgn}(\sigma_{ei}) = \begin{cases} -1, & \text{if } \sigma_{ei} < 0, \\ 1, & \text{if } \sigma_{ei} > 0. \end{cases}$$

As  $\varepsilon_2$  approaches zero, the rotation angle  $\theta(t)$  can be driven arbitrarily close to  $2\pi$  if the initial value  $\theta(0)$  of  $\theta(t)$  is larger than  $\pi$ .

The advantage of the proposed UFSMC law (32) is that the unwinding phenomenon is avoided during the rigid spacecraft attitude maneuver, and the disturbance is compensated by the designed controller.

## IV. SIMULATION

In this section, simulations are conducted to demonstrate the performance of the presented UFSMC law (32) for rest-to-rest attitude maneuvers of a rigid spacecraft. In addition, the SMC controller in [16] is adopted for comparison.

### A. Simulation Settings

1) *Spacecraft parameter values:* The inertia matrix of the rigid spacecraft is  $J = \text{diag}[114 \ 86 \ 87] \text{ kg} \cdot \text{m}^2$ . The initial values of the attitude velocity  $\omega$  and attitude  $\sigma$  are  $\omega(0) = [0 \ 0 \ 0]^T$  and  $\sigma(0) = [0 \ 0 \ 0]^T$ , respectively. The disturbance is  $d = 10^{-2} \times [\sin(0.05t) \ 0.5 \sin(0.05t) \ -\cos(0.05t)]^T$ .

2) *Controller parameter values:* The tuning parameters of the proposed UFSMC law (32) are chosen as

$$\alpha = 2, \gamma_1 = 30, \varepsilon_1 = 0.5, \varepsilon_2 = 0.0001.$$

In addition,  $\gamma_2(t)$  is obtained from (33). The parameters of the SMC controller [16] are chosen as,

$$k = 1.5, \lambda = -0.5, \varepsilon = 0.5.$$

3) *Control goal:* The control goal is to perform two rest-to-rest attitude maneuvers for the rigid spacecraft with system parameters given in Section IV-A1. Two different scenarios of desired attitude values are given as follows.

Scenario A. The desired attitude and angular velocity are  $\sigma_d = [0.1 \ 0.2 \ -0.3]^T$ , and  $\omega_d = [0 \ 0 \ 0]^T \text{ rad/s}$ , respectively.

Scenario B. The desired attitude and angular velocity are  $\sigma_d = [0.7809 \ 0.4685 \ -0.7809]^T$ , and  $\omega_d = [0 \ 0 \ 0]^T \text{ rad/s}$ , respectively.

In Scenario A, it can be obtained from (3) that  $\sigma_e(0) = [0.1 \ 0.2 \ -0.3]^T$ . Further, there holds  $\theta(0) = 1.4321 < \pi$  according to (8). Thus,  $\theta(t) = 0$  is the nearest equilibrium. The controller needs to guarantee that  $\theta(t)$  decreases to zero monotonically. In Scenario B, it can be obtained from (3) that  $\sigma_e(0) = [0.7809 \ 0.4685 \ -0.7809]^T$ . Further, there holds  $\theta(0) = 3.5036 > \pi$  according to (8). Thus, the spacecraft needs to rotate 3.5036 rad to reach the desired attitude if only  $\theta(t) = 0$  is chosen as the equilibrium. However, the spacecraft only needs to rotate 2.7796 rad if  $\theta(t) = 2\pi$  is also considered as an equilibrium.

### B. Simulation results

1) *Simulation results for Scenario A:* The SMC controller in [16] and proposed UFSMC law (32) are adopted to do simulations for Scenario A. The simulation results are shown in Fig. 1.

The response of  $\theta(t)$  and angular velocity error  $\omega_{ei}$ ,  $i = 1, 2, 3$  are shown in Fig. 1(a) and Fig. 1(b), respectively. It can be seen from Fig. 1(a) and Fig. 1(b) that  $\theta(t)$  and the angular velocity errors of the system (7) converge to 0 in about 6s by adopting the proposed UFSMC law (32), while the SMC controller needs 12s. The spacecraft attitude responses using Euler angles, i.e., Roll, Pitch, and Yaw, are shown in Fig. 1(c), which indicates that the attitude maneuver problem is effectively settled by the controller UFSMC law (32) and SMC law. The time evolution of control torques  $u_i$ ,  $i = 1, 2, 3$  are shown in Fig. 1(d). The control torque of the proposed UFSMC law (32) is smaller than that of the SMC controller.

In conclusion, the UFSMC controller can obtain higher pointing accuracy and better stability in a shorter time.

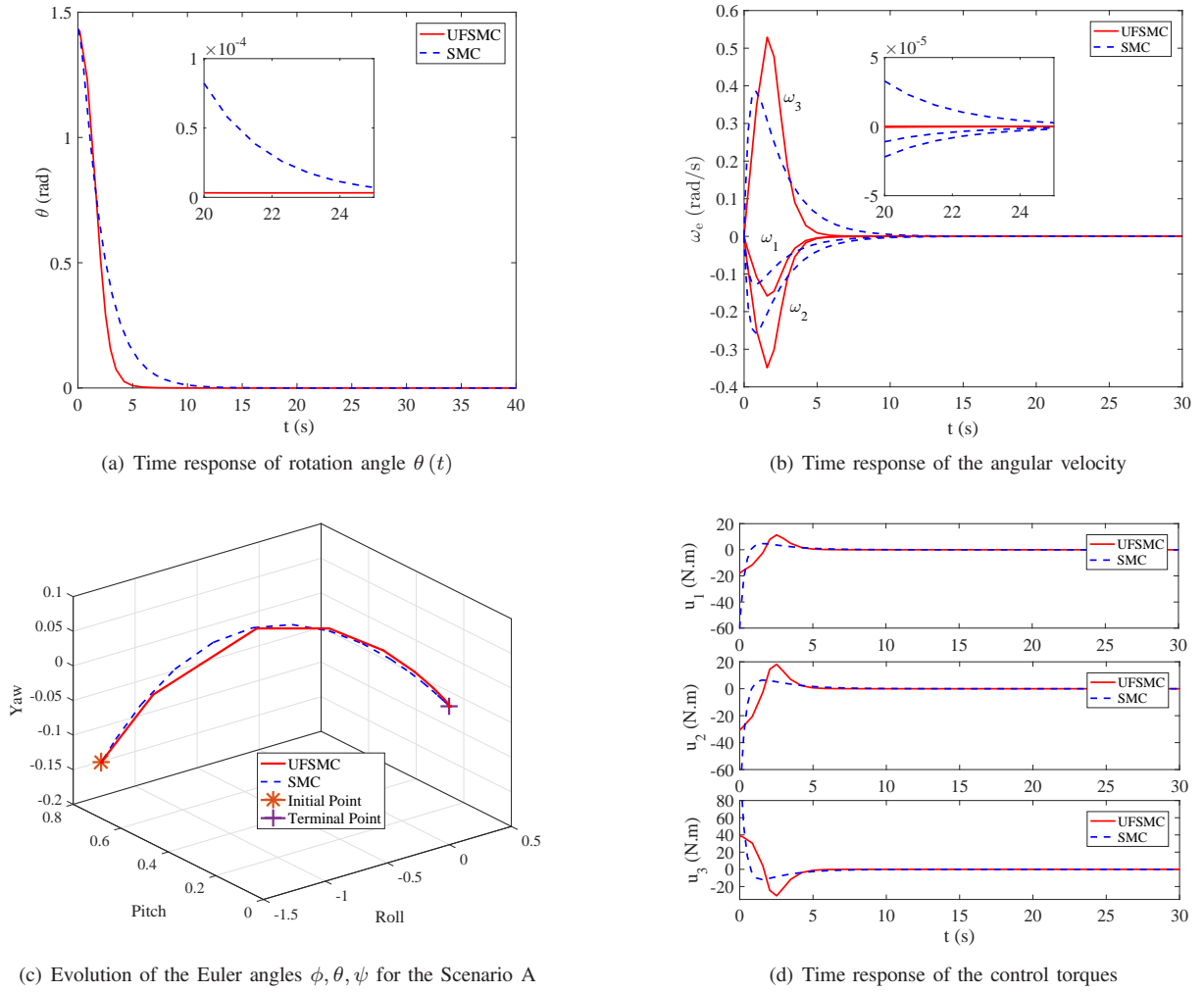


Fig. 1: Comparison results of UFSMC law (32) and SMC [16] for Scenario A

2) *Simulation results for Scenario B:* The SMC controller in [16], and the proposed UFSMC law (32) are adopted to do simulations for Scenario B. The simulation results are summarized in Fig. 2.

The response of the rotation angle  $\theta(t)$  is shown in Fig. 2(a). The principle rotation angle  $\theta(t)$  converges to 0 in about 14s by adopting the SMC controller in [16], while  $\theta(t)$  converges to  $2\pi$  in about 6s by adopting the proposed UFSMC (32). This means that the rigid spacecraft needs to rotate 3.5036 to reach the desired attitude under the controller SMC in [16], while the rigid spacecraft only needs to rotate 2.77 to reach the desired attitude under the proposed UFSMC (32). The behavior of angular velocity error  $\omega_{ei}, i = 1, 2, 3$  is shown in Fig. 2(b). It can be observed from Fig. 2(b) that the attitude velocity of the rigid spacecraft (7) converges to 0 in about 6s by using the proposed UFSMC law (32), while the SMC law needs a longer time. The spacecraft attitude responses using Euler angles, i.e., Roll, Pitch, and Yaw, are the roll, pitch, and yaw angles, respectively) are shown in Fig. 2(c). The maneuver angle of the UFSMC law (32) is smaller than that of SMC law. This means that the presented UFSMC law (32) can avoid the unwinding phenomenon successfully, but the SMC controller can not. The control torques  $u_i, i = 1, 2, 3$  are shown in Fig. 2(d), which indicates that the attitude maneuver is effectively settled by the UFSMC law(32) and SMC controller. It can also be observed that the control torque of the proposed control law is less than that of the SMC controller.

In conclusion, the proposed UFSMC controller (32) satisfies the control objective described in Section II-D, and it achieves higher pointing accuracy and better stability in a shorter time compared with the SMC controller (32).

## V. CONCLUSION

In this paper, an unwinding-free sliding mode control law is presented for the attitude maneuver control of a rigid spacecraft. By constructing a new switching function, the unwinding-free property of the closed-loop attitude maneuver control system of a rigid spacecraft is ensured when the system states are on the sliding surface. Furthermore, by designing a sliding mode control law with a dynamic parameter, the unwinding-free performance of the closed-loop attitude maneuver control system of a rigid spacecraft is guaranteed before the system states reach the sliding surface. In addition, the switching function converges to zero in finite-time by the developed control scheme. Finally, a numerical simulation is conducted to demonstrate the effectiveness of the developed control law. The simulation results show that the unwinding phenomenon is avoided by adopting the designed switching surface and controller.

## REFERENCES

- [1] P. C. Hughes, *Spacecraft attitude dynamics*. Courier Corporation, 2012.
- [2] R. Sharma and A. Tewari, "Optimal nonlinear tracking of spacecraft attitude maneuvers," *IEEE Transactions on Control Systems Technology*, vol. 12, no. 5, pp. 677–682, 2004.

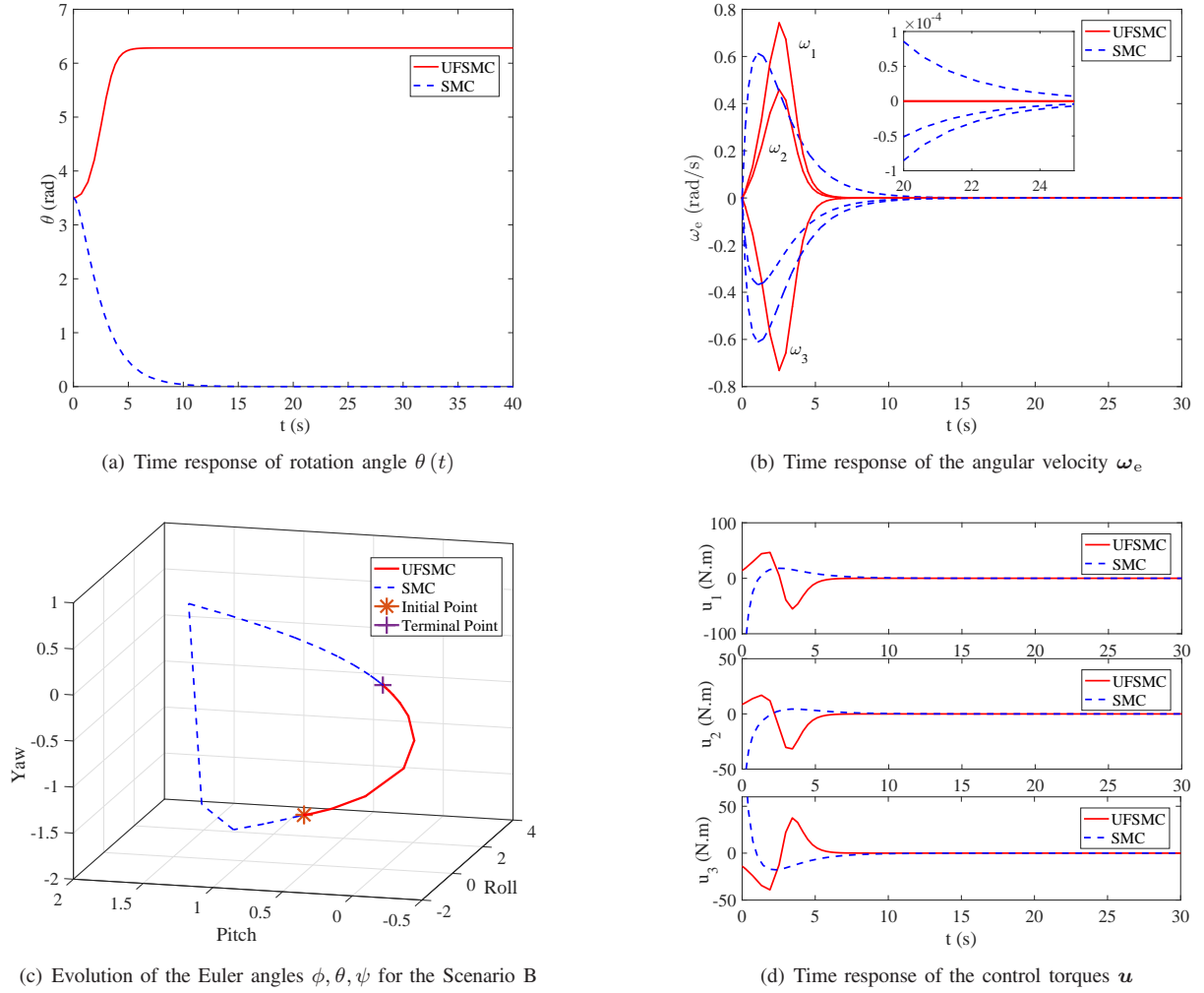


Fig. 2: Comparison results of UFSMC law (32) and SMC [16] and for Scenario B

- [3] S. M. Amrr, M. U. Nabi, and A. Iqbal, "An event-triggered robust attitude control of flexible spacecraft with modified Rodrigues parameters under limited communication," *IEEE Access*, vol. 7, pp. 93198–93211, 2019.
- [4] R. Jin, X. Chen, Y. Geng, and Z. Hou, "Lpv gain-scheduled attitude control for satellite with time-varying inertia," *Aerospace Science and Technology*, vol. 80, pp. 424–432, 2018.
- [5] F. Bayat, "Model predictive sliding control for finite-time three-axis spacecraft attitude tracking," *IEEE Transactions on Industrial Electronics*, vol. 66, no. 10, pp. 7986–7996, 2018.
- [6] N. Ji and J. Liu, "Vibration control for a flexible satellite with input constraint based on nussbaum function via backstepping method," *Aerospace Science and Technology*, vol. 77, pp. 563–572, 2018.
- [7] Y. P. Chen and S. C. Lo, "Sliding-mode controller design for spacecraft attitude tracking maneuvers," *IEEE Transactions on Aerospace and Electronic Systems*, vol. 29, no. 4, pp. 1328–1333, 1993.
- [8] P. M. Tiwari, S. Janardhanan, and M. Nabi, "Attitude control using higher order sliding mode," *Aerospace Science and Technology*, vol. 54, pp. 108–113, 2016.
- [9] A. Wu, R. Dong, Y. Zhang, and L. He, "Adaptive sliding mode control laws for attitude stabilization of flexible spacecraft with inertia uncertainty," *IEEE Access*, vol. 7, pp. 7159–7175, 2018.
- [10] A.-M. Zou, K. D. Kumar, Z.-G. Hou, and X. Liu, "Finite-time attitude tracking control for spacecraft using terminal sliding mode and chebyshev neural network," *IEEE Transactions on Systems, Man, and Cybernetics, Part B (Cybernetics)*, vol. 41, no. 4, pp. 950–963, 2011.
- [11] S. S.-D. Xu, C.-C. Chen, and Z.-L. Wu, "Study of nonsingular fast terminal sliding-mode fault-tolerant control," *IEEE Transactions on Industrial Electronics*, vol. 62, no. 6, pp. 3906–3913, 2015.
- [12] N. A. Chaturvedi, A. K. Sanyal, and N. H. McClamroch, "Rigid-body attitude control," *IEEE control systems magazine*, vol. 31, no. 3, pp. 30–51, 2011.
- [13] H. Du, S. Li, and C. Qian, "Finite-time attitude tracking control of spacecraft with application to attitude synchronization," *IEEE Transactions on Automatic Control*, vol. 56, no. 11, pp. 2711–2717, 2011.
- [14] P. Tsiotras, "Further passivity results for the attitude control problem," *IEEE Transactions on Automatic Control*, vol. 43, no. 11, pp. 1597–1600, 1998.
- [15] B. Cong, X. Liu, and Z. Chen, "Backstepping based adaptive sliding mode control for spacecraft attitude maneuvers," *Aerospace Science and Technology*, vol. 30, no. 1, pp. 1–7, 2013.
- [16] J. L. Crassidis and F. L. Markley, "Sliding mode control using modified Rodrigues parameters," *Journal of Guidance, Control, and Dynamics*, vol. 19, no. 6, pp. 1381–1383, 1996.
- [17] M. D. Shuster *et al.*, "A survey of attitude representations," *Navigation*, vol. 8, no. 9, pp. 439–517, 1993.